Dosimetri för PCI-behandling av cancertumörer - Populärvetenskaplig sammanfattning

Linnea Rading

År 2008 orsakade olika former av cancer 13 % av alla dödsfall i världen. Det gör cancer till den vanligaste dödsorsaken i I-länder. Bröstcancer är den vanligaste cancerformen hos kvinnor medans lungcancer är vanligast bland männen. De vanligaste behandlingssätten är kirurgi, strålning och kemoterapi (cellgifter).

PCI, som är en förkortning för engelskans Photo Chemical Interraction, är en ny metod som man hoppas ska bidra till att bota fler av dem som drabbas.

När mediciner ges, som t.ex. cellgifter mot cancer, är det viktigt att medicinen kan levereras dit den gör nytta. Många mediciner måste komma in i cellen för att verka. Små molekyler kan diffundera in igenom cellväggen men större molekyler tas ofta upp av cellen, genom vad som kallas endosytos, och förstörs eftersom cellen inte känner igen substansen. PCI använder ljus för att öppna upp en väg in genom cellmembranet för dessa stora molekyler.

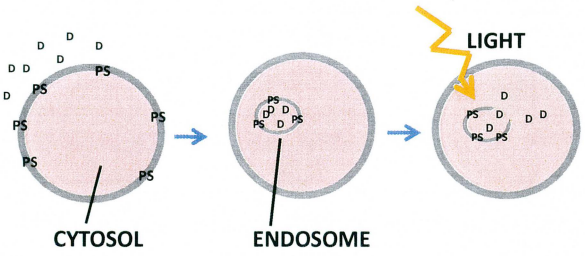

Figure 1: Schematisk bild på hur en medicin kan ta sig in i cellen med hjälp av PCI-teknik. D är medicinen som ska levereras och PS står för fotosensibiliseraren.

PCI-effekten bygger på samverkan mellan en så kallad fotosensibiliserare, syre och ljus av rätt våglängd. Fotosensibiliseraren och ljuset kan tillsammans få syre att bli reaktivt och den reaktiva molekylen förstör sin närmaste omgivning. Den fotosensibiliseraren som är utvecklad för PCI fäster i cellmembranet. Medicinen som man vill leverera till cellen omsluts av cellmembranet och dras in i cellen i så kallade endosomer. När man lyser på cellerna så kommer endosomernas väggar att spricka och medicinen som man vill leverera kan ta sig ut.

Vad är det för molekyler som man vill leverera? Genterapi är en ny behandlingsmetod som går ut på att man vill ta bort eller tillsätta gener till cellerna. Metoden har länge verkat lovande, men problemet har varit att man inte har ett bra sätt att leverera de stora molekylerna. För genterapin kan PCI-tekniken spela en viktig roll. Även upptaget för mindre molekyler, som cellgifter, kan ökas med hjälp av PCI-tekniken och behandlingen kan då bli effektivare.

PCI-effekten beror på hur mycket syre och fotosensibiliserare som finns i vävnaden men också på hur mycket man belyser cellerna. Sambandet mellan de tre komponenterna är komplext och vanligtvis så koncentrerar man sig på att beräkna ljusdosen och antar att mängden syre och fotosensibiliserare är konstant. För att veta hur mycket ljus en viss del av en tumör har fått måste man veta hur ljuset utbreder sig i vävnaden. När ljus utbreder sig i vävnad kan det både spridas och absorberas och hur det sprids och absorberas bestäms av vävnades optiska egenskaper.

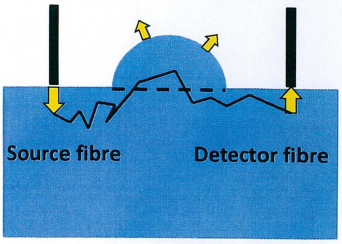

Figure 2: Vid en mätning går ljuset mellan källfibern och flera detektionsfiber. På vägen kan ljuset spridas, absorberas eller lämna vävnaden.

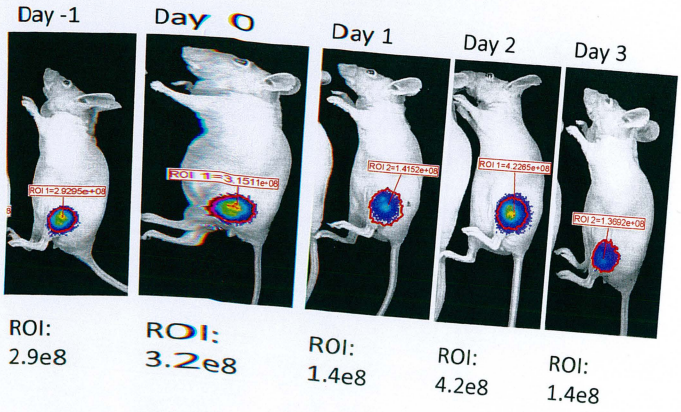

Figure 3: Mössen fotograferas flera dagar i följd och ROI-värdet är ett mått på hur mycket blodförsörjning tumören har

Spectra Cure är med i ett samarbete med två andra företag. Samarbetsprojektet går ut på att under tre år testa och utveckla PCI-tekniken. Tekniken ska först testas på möss för att visa att det går att leverera olika molekyler till cellerna och för att bestämma vilka ljusdoser som behövs. Är djurstudierna lyckade kommer tekniken att testas på människor. Spectra Cures del i projektet är att tillhandahålla ett system som kan behandla både ytliga tumörer och tumörer inuti kroppen. Systemet ska dessutom kunna mäta de optiska storheterna i vävnaden. Systemet som används har tre behandlingsfiber och fem mätfibrer.

Systemet har testats på fantomer som är flytande vätskor med liknande optiska egenskaper som vävnad har. De optiska egenskaperna är kända och fantomerna kan därför användas som referens. För att uppskatta de optiska egenskaperna gissar man först de optiska egenskaperna och simulerar från dem fram en ljusdos. Den framsimulerade ljusdosen jämförs med den uppmätta och gissningen justeras. Proceduren upprepas tills den simulerade ljusdosen motsvarar den verkliga. Systemet kunde med bra precision uppskatta de optiska storheterna hos olika fantomer.

Systemet testades även på möss på Radiumhospitalet i Norge. Målet är att förstå hur PCI-effekten beror på ljusdosen och bestämma en ljusdos som ger maximal PCI-effekt. När mössen är behandlade så följs de under tre dagar för att se hur tumören utvecklas. Att mäta optiska storheter på möss är svårt av flera anledningar. Mössen är små och har en komplicerad geometri vilket gör att de vanligaste modellerna för ljussimulering ger felaktiga resultat. Mössen rör sig under behandlingen och det är därmed svårt att bibehålla kontakten mellan fibrerna och musen. Trots svårigheterna gav mätningarna rimliga resultat.

Abstract

PCI (Photo Chemical Internalization) is a new method that, by combining a drug called a photosensitizer with light, opens for the possibility to deliver large molecules to the inside of the cell. The method offers the possibility to use drugs that consists of large molecules but it also makes it possible to only deliver the drug to the part of the body that is irradiated. Chemotherapy is a common treatment for cancer but it has severe side effects. With PCI, only the tumour is irradiated and the severe side effects in the rest of the body can hopefully be avoided.

This master thesis is a part of a project involving three companies, PCIBiotech, siRNAsense and SpectraCure. The goal for the project is to develop and test the PCI-technique in pre-clinical and clinical trials. Spectra Cure's part of the project is to provide with the illumination device and to contribute with the dose planning.

In PCI it is of ample importance to control the light dose given to the tumour. The light dose given depends on the optical properties of the tissue but also on the geometry and position of the tumour. The illumination device provided by Spectra Cure has the possibility to illuminate the tumour but also to measure the optical properties.

In this master thesis, simulations and experiments are performed in order to learn how to best deliver the light and at the same time measure the optical properties. The system is tested on tissue phantoms and on mice. The results from the evaluation of the optical properties are presented and also some preliminary results from the first treatment using the PCI-technique.

Contents

Chapter 1

Introduction to PCI-dosimetry with SpectraCure's light delivery system

PCI (Photo Chemical Internalization) is a new method that, by combining a drug called a photosensitizer with light, opens for the possibility to deliver larger molecules to the inside of the cell. Why is it so important to deliver large molecules to the cell?

Drugs act in different ways, some act from the outside of the cell but some have to get through the cell membrane to be efficient. Smaller molecules can diffuse through the cell membrane but larger molecules cannot enter the cell without being degraded.

The lack of a method to efficiently deliver large molecules to the cell is a huge problem in the new branch of treatment called gene therapy. Gene therapy is a treatment where new genes are inserted into the organism. The goal is to correct a gene that is responsible for a disease. Gene therapy has a great potential but the problem is to deliver the large DNA-molecules to the cells and also to deliver the DNA to the correct site of the gene. The development of Gene therapy is focused on treating diseases where only one defect gene is the cause of the disease, Haemophilia and Cystic fibrosis are two such examples. Gene therapy is also promising in cancer treatment where the relatively newly discovered siRNA (silencing RNA) has been shown to stop tumour growth *in vitro*. When the goal of the gene therapy is to treat a specific area of the body, the PCI-techniqe might bring the solution.

The PCI-technique also has the potential to reduce the doses of drugs already in use in various therapies and thus avoid severe side effects.

1.1 The Eurostars project

Three companies (SiRNAsense, PCI Biotech and SpectraCure) in Norway and Sweden are collaborating in the Eurostars project. The Eurostars project aims at developing a method for delivery of silencing RNA (siRNA) to tumours. siRNA can be designed to target proteins that are altered in the cancer tumour. By targeting specific proteins, the severe side effects of many cancer therapies can hopefully be avoided. The potential of siRNA has been known for several years; but the potential has not yet been realized. A main reason is the lack of an efficient way of delivering the large molecules. PCI Biotech has developed a technology, PCI (Photo Chemical Internalization), for light induced delivery of drugs. The PCI technique will be further described in Chapter 3.

In the Eurostars project, the potential of siRNA as a drug will be combined with the PCI technology for drug delivery. PCI is a technology based on the use of a light source in combination with a photosensitizer. The light will interact with the photosensitizer and a path of drug delivery into the cell is opened. SpectraCure's part of the project is to provide an instrument for controlled light delivery. The instrument will be adopted to animal studies and, further ahead, for clinical trials on humans.

For efficient use of the PCI-technology it is important to be able to control the light dose delivered to the tumour. The light dose depends on the optical properties of the tissue and the SpectraCure instrument will, apart from delivering the light, measure the optical properties and provide dosimetry feed-back for each individual treatment.

1.2 Outline and goal of the master thesis

Spectra Cure's role in the current part of the Eurostars project is to provide a system that can illuminate the tissue and at the same time measure the optical properties. A comprehension of how light propagate in tissue is important and an explanation will be given in Chapter 2. The PCI technology is briefly described in Chapter 3 and the goal with the chapter is to provide a comprehensive overview of the technology since it is an unknown area for most physicists. In Chapter 4 the system will be discussed from a technical point of view in order to understand the possibilities and limitations of the system.

In Chapter 5 and Chapter 6 the simulations and the experiments are described. Chapter 5 provides an overview of the dosimetry in order to understand how all the components contribute to in the end deliver a light dose that will cure the cancer. The different parts such as the positioning of the optical fibres, the geometry and the theoretical model for light propagation are discussed in detail. In Chapter 6 tissue phantoms with known optical properties are used to evaluate the system. The results are analysed using different theoretical models.

This chapter is important since the knowledge and experience gained in how to perform measurements and how to evaluate the result will be used in the mouse study in the Eurostars project.

Chapter 7 is about the preclinical trials in Norway. The technical work done for the preclinical study is described. Some preliminary result will be presented but the full evaluation of the result from the study is outside the scope of the master thesis due to time constraints. The last chapter, Chapter 8, is devoted to conclusions and a discussion of the continuation of the Eurostars project.

Chapter 2

Theory of light propagation in biological tissue

To be able to simulate how the light propagates is of uttermost importance for a successful PCI or PDT treatment. This is not only true for PCI and PDT treatment but for all treatments and diagnostic methods that involve light. I will give some examples:

- Using a laser instead of a scalpel in surgery. This is common in neurosurgery and vascular surgery.
- Treating for example astigmatism by changing the shape of the cornea with a laser.
- OTC - Optical coherence tomography is used to get 3D pictures of the retina in the eye.
- Research is conducted to find out if optical methods could replace, or be a complement to, mammography.

In the different treatments, the outcome is strongly dependant on the light dose that reaches the biological tissue to be treated. In diagnostics, it is important to know where the photons have travelled in order to form a picture of, for example, breast tissue. This chapter will describe and explain the theory of light propagation and which models that we can use in order to simulate how the light propagates. I will also discuss how the optical properties of tissue can be estimated.

2.1 Optical properties in biological tissue

When light travels in biological tissue it can be scattered and absorbed. Typical for biological tissue is that the probability for light in the visible wavelength

regime to be scattered is much higher than the probability to be absorbed. The scattering is described by two physical quantities, the scattering coefficient $\mu_s[m^{-1}]$ and the g-factor. The scattering coefficient tells us the probability of scattering per unit length and the g-factor tells us in which direction the photons, in average, will be scattered. Isotropic scattering has a g-value of zero while g=1 means totally forward scattering. The two quantities are often combined to the reduced scattering coefficient $\mu_s' = (1-g)\mu_s$. The absorption is described by $\mu_a[m^{-1}]$ and $\frac{1}{\mu_a}$ can be interpreted as the mean distance a photon travels before it gets absorbed.

2.2 How to simulate the light propagation

When simulating light transport in tissue, the goal is to know the fluence rate, $\phi(\mathbf{r},t)[W/m^2]$, in the whole geometry of interest. This simulation is referred to as the forward model. ϕ can be understood as the energy per time carried by photons through the mantel surface of a small sphere. In the following equations the radiance $L(\mathbf{r},\mathbf{s},t)$ is often used and the radiance is related to the fluence rate through $\phi(\mathbf{r},t) = \int_{4\pi} L(\mathbf{r},\mathbf{s},t)d\omega$. Photons propagating in scattering media are described by the Radiative Transport Equation (RTE). The RTE describes the alterations of radiance in a small volume dV and is given by:

$$\frac{1}{c}\frac{\partial L(\mathbf{r},\mathbf{s},t)}{\partial t} = -\mathbf{s}\cdot\nabla L(\mathbf{r},\mathbf{s},t) - (\mu_s+\mu_a)L(\mathbf{r},s,t) + \mu_s\int_{4\pi} p(\mathbf{s},\mathbf{s}')L(\mathbf{r},\mathbf{s}',t)d\omega' + q(\mathbf{r},\mathbf{s},t) \tag{2.2.1}$$

$L(\mathbf{r},\mathbf{s},t)$ [$\mathrm{Wcm^{-2}sr^{-1}}$] denotes the irradiance of light in position $\mathbf{r}$ going in direction $\mathbf{s}$, $q(\mathbf{r},\mathbf{s},t)$ is the source term, c denoting the speed of light in the medium and $p(\mathbf{s},\mathbf{s}')$ is the phase function that describes the probability of a photon scattering from $\mathbf{s}'$ to $\mathbf{s}$. Equation (2.2.1) describes the conservation of radiance for a certain direction. The term on the left hand describes how the number of photons travelling in direction $\mathbf{s}$ at position $\mathbf{r}$ changes over time due to the terms at the right hand side describing absorption, scattering into and out of the direction $\mathbf{s}$, boundaries and sources. For more details, see [1] and doctoral theses from the Medical Optics group at the atomic division at Lund University, [2], [3].

2.2.1 The diffuse approximation of the RTE

The RTE can be solved by numerical methods or by statistical methods such as the Monte Carlo method. If it is possible to find an analytical solution, it would be of interest since it requires much less computational power. The RTE contains too many unknown to be solvable analytically in a general case. A common approach is to simplify the problem by using different approximations and I will use the diffuse approximation (DE) in this master thesis. I will

not derive the DE from the RTE but I will discuss the approximations that are made and the limitations of the diffuse approximation. It is important to remember that the model that is used almost through-out the master thesis is an approximation and must be used under the conditions where the approximation is valid.

In the diffuse approximation, L(**r**,**s**,t), q(**r**,**s**,t) and p(**s**,**s**') is expanded in spherical harmonics, but the series are truncated after the linear term. This approximation implies that only diffuse light can be described by the function. One more assumption is to be made;

$$\mu_s' >> \mu_a \tag{2.2.2}$$

With those approximations the DE yields:

$$\begin{aligned} \frac{1}{c}\frac{\partial\phi(\mathbf{r},t)}{\partial t} - \nabla\cdot(D(\mathbf{r})\nabla\phi(\mathbf{r},t)) \\ + \mu_a\phi(\mathbf{r},t) = S_0(\mathbf{r},t) \end{aligned} \tag{2.2.3}$$

D is the diffusion coefficient and is often defined as:

$$D = \frac{1}{3(\mu_a + \mu_s')} \tag{2.2.4}$$

The RTE is now simplified through approximations and can be solved either analytically by Green's solution or numerically using i.e. Finite Element Method (FEM). The analytic method requires less computational power but is restricted to simple geometries and homogeneous optical properties.

The easiest case to solve analytically is an isotropic point source sending out a short pulse in an infinite medium, see (2.2.5). In reality this represents the situation where an interstitial fibre is inserted deep into the body and the surroundings are considered to be homogeneous. This forward model is used in Spectra Cure's newest system called P18, which is designed to treat prostate cancer.

$$\phi(r,t) = \left(\frac{E}{4\pi Dct}\right)^{3/2} e^{-\mu_a ct} e^{-\frac{r^2}{4Dct}} \tag{2.2.5}$$

If the light source irradiates for a long time, the steady state solution is of interest and is given by:

$$\phi(r) = \frac{E}{4\pi Dr} e^{-\mu_{eff} r} \tag{2.2.6}$$

where

$$\mu_{eff} = \sqrt{\mu_a(\mu_a + \mu_s')} \tag{2.2.7}$$

is the effective attenuation coefficient.

By introducing boundary conditions, the solution can be extended to slab and half infinite geometries. Close to a boundary, the fluence rate is lower due to that photons passing through the boundary cannot be scattered back. To simulate this situation, an imaginary negative source is introduced at a distance $2z_b + z_0$ from the boundary. See figure 2.1. This leads to that the fluence rate is zero at an extrapolated boundary z_b from the physical boundary. The reason to choose the fluence rate to be zero not at the boundary but at z_b from the boundary is partly because of the Fresnel reflection at the boundary. Not all photons will pass the boundary; some will be reflected back due to the mismatching in refractive indexes and contribute to that the fluence rate is non-zero at the boundary. The distance to the extrapolated boundary, z_b, is important since it decides how well the analytical model can describe the real physical situation. In Haskell et al. [4], an approximate expression for z_b is given:

$$z_b = \frac{1 + R_{eff}}{1 - R_{eff}} \frac{2}{3} l_{tr} \tag{2.2.8}$$

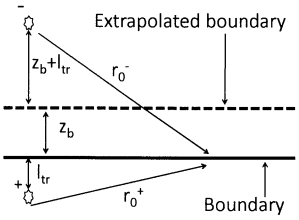

Figure 2.1: The extrapolated boundary model with the real source and the imaginary source

where $l_{tr} = 1/\mu_s'$ is the transport mean free path. R_{eff} is the fraction of emittance that is reflected and becomes the irradiance. If the refractive index outside the medium is the same as the refractive index inside the medium, there will be no Fresnell reflection and $R_{eff} = 0$. This will lead to $z_b = 2/3l_{tr}$. If the boundary is between flesh (n=1.4) and air (n=1), $R_{eff} = 0.493$ and $z_b = 2.18$ mm for $\mu_s' = 0.9$ mm^{-1}. R_{eff} is obtained by integrating the Fresnel reflection, for exact formulation see [4].

Equation (2.2.6) is now extended with an extra term for the negative source.

$$\phi(r) = \frac{1}{4\pi D} \left(\frac{exp(-\mu_{eff} r_0^+)}{r_0^+} - \frac{exp(-\mu_{eff} r_0^-)}{r_0^-} \right) \tag{2.2.9}$$

where r_0^+ and r_0^- are the distances to the real source and the imaginary source respectively.

For non-invasive measurements, it it the reflected light, from example the skin that is measured. In literature, different models are used, [5] [6]. Either the reflected light is described by the flux at the boundary or as a combination of the flux and the fluence rate. The fluence rate is described in equation 2.2.9 and the flux is given by:

$$R_f(\rho) = -D\nabla\phi(\rho, z) * (-\mathbf{z})|_{z=0} \tag{2.2.10}$$

2.2.2 Solving the RTE with a Monte Carlo simulation

The diffusion equation is derived from the RTE and can be solved either analytically or numerically i.e. by the Finite Element Method. The diffusion equation imposes constraints on the optical properties, distance from the source and the type of source. If the RTE can be solved directly those constraints can be avoided. The Monte Carlo method is a statistical method that simulates the

propagation of each photon. A very good and step by step explanation of Monte Carlo method is provided by Prahl in ref. [7] and only a brief introduction will be presented here.

In principle each photon path is simulated separately but to speed up the simulation, a package of photons is used. For every iteration, the photon package will take one step in a direction decided by μ_s and with a length decided by μ_s and μ_a. The step and the angle are not fixed, but are decided using a random variable in order to have a distribution that follows the probability density function for the angle or the length. At each displacement, the weight of the package is reduced due to absorption and it is controlled that the photon is still inside the medium. If the photon leaves the medium, the photon will either be transmitted or internally reflected with the same probability as in the real situation.

The Monte Carlo approach will result in a more accurate solution compared to when the diffusion approximation is used. Why do we not always use the Monte Carlo method? Since it is a statistical method, it requires many photons for a correct result. Only a small number of the photons will reach a point far from the source and the requirement of sufficient photons cannot always be met due to limited computing capacity. Each photon is independent of the other photons and hence the problem can be solved in parallel. The Biophotonic group in Lund has used the parallelism of GPUs to speed up the calculations [8]. This technique, in combination with faster computers, is promising for the Monte Carlo method.

2.3 How to measure optical properties

In the previous section it is discussed how to model the light propagation. The optical properties, the geometry and the sources were known and it was the fluence rate, ϕ, that were sought at every position in the geometry. This is called the forward model. In a treatment, the optical properties are often not known and they can vary significantly between patients and also within the treatment volume. There is a need for methods to measure the optical properties. Direct or indirect measurements of the fluence rate inside or outside the geometry reflects the optical properties of the tissue. The goal is to find the optical properties that, when used in the forward model, give the same fluence rate as the measurements. This is called the inverse problem.

2.3.1 Spatially resolved measurements

With some rearrangement, the steady state solution to the diffusion equation in an infinite medium can be written as:

$$\ln(\phi r) = \ln(\frac{P}{4\pi D}) - \mu_{eff} r \tag{2.3.1}$$

The equation describes a straight line if $\ln(\phi r)$ is plotted against r. If measurements taken at different distances are plotted into this diagram a line can be

fitted and the gradient gives the μ_{eff}. D can be retrieved from the intersection with the y-axis. When D and μ_{eff} is known, μ_a and μ_s' can be calculated.

The light that is measured is proportional to ϕ and to retrieve the proportionality constant absolute calibration is needed. Direct calibration is hard to do and the result is often erroneous. To retrieve μ_{eff} the absence of direct measurements is not important since the proportionality constant shifts the line vertically, thus not affecting the slope of the line. On the other hand, it is a problem when retrieving D since it affects the intersection with the y-axis. An approach is to be content with extracting μ_{eff} and retrieving one of μ_a or μ_s' by using prior knowledge of the other.

The method to obtain the optical properties described above uses the steady state solution to the diffusion equation as the forward model. What if the geometry is more complicated, what forward model can be used in this case? As described in section 2.2.1 the diffusion equation can also be solved for half infinite and slab geometries by introducing imaginary sources. If the geometry is even more complicated, a FEM-model can be used to simulate the light. In this case it is also possible to assign different optical properties to different parts of the tissue. It can for example be of interest to distinguish between the tumor tissue and the surrounding tissue. It is an iterative process to find the best fit between the simulated measurements and the real measurements. This is the drawback since, for every iteration, a FEM-simulation is performed and it is time consuming. It is also possible to use Monte Carlo as the forward model; this is preferred in smaller geometries since there are no limitations on the distance from the source. The Monte Carlo method has the same drawbacks as FEM since it requires considerable computational power.

In all spatially resolved measurements the distance between the measurement points and the source needs to be spread out in an interval. No measurement point should be closer than approximately 5mm since the light is not diffuse that close to the source and hence the diffusion approximation is not valid. The longest distance between the source and the detector is not limited by the diffusion approximation but by the detectors ability to measure weak signals and the Signal To Noise (SNR) ratio and the size of the probed tissue.

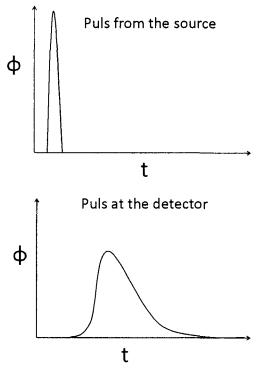

Figure 2.2: Schematic picture of the pulse broadening

2.3.2 Time of flight measurements

In Time Of Flight (TOF) measurements the light is collected at one fixed source-detector distance instead of several as in the spatially resolved method. A short pulse is emitted from the source and the photons have been scattered several times before reaching the detector. This result in a broadening of the pulse, see figure 2.2. The shape of the pulse depends on the optical properties. An increased scattering delays the pulse since the photons have travelled a longer distance whereas an increased absorption changes the shape of the slope. The fact that changes in the optical properties give rise to different effects on the shape of the curve means that the TOF-method can separate μ_a and μ_s'. Either analytical expressions or Monte Carlo simulations can be used as the forward model for simple geometries, but Monte Carlo has shown to give more accurate

result [9]. The inverse problem consists in fitting the experimental curve to the forward model.

Chapter 3

Photo Chemical Internalization - PCI

When treating diseases with drugs, it is important to be able to deliver the drug to the inside, called the cytosol, of the cell. If the drug consists of small molecules it can diffuse into the cell, but this is not possible for bigger molecules. Many drugs, for example chemotherapeutic agents, cannot penetrate the cell membrane efficiently. This leads to a treatment where higher drug doses must be used and the negative side effects will be stronger. A new method named Photo Chemical Internalization (PCI) solves the problem by using light and a photosensitizer. The drug to be delivered is taken up by the cell and encapsulated in vesicles containing a photosensitizer. When the vesicle is irradiated, the photochemical reaction between the light and the photosensitizer leads to rupture of the vesicle and the drug is released into the cytosol of the cell.

Instead of using the photochemical reaction as a mean to deliver a drug, the reaction can be used to cause necrosis (e.g. cell death) directly to the cell. This method is called PDT (Photo Dynamic Therapy) and is commonly used in cancer treatment.

3.1 Photodynamic Therapy - PDT

PDT is an important part of PCI and a short description will be provided here. For more information, see the following PhD theses: [10], [11] and [2]. When light of a specific wavelength reacts with a photosensitizer, the photosensitizer is excited. The photoensitizer molecule can either relax to the ground state or into a triplet state. The triplet state has a long lifetime and the photosensitizer molecule can react and excite the oxygen in the tissue. Among other possible reactions, highly reactive singlet oxygen ($^1O_2$) can be formed. Singlet oxygen will react with its direct surroundings causing changes in the intra-cellular structures. In PDT, the goal is to cause changes in the structure such that the cell dies. If this can be achieved for all cells in a tumour, the cancer can be treated.

PDT is, for example, used in clinics for treating a type of skin cancer called basel cell cardionoma. Several clinical studies are ongoing with the goal to cure cancer through PDT. Spectra Cure is currently planning for a phase two clinical study of prostate cancer.

3.2 PCI

Large molecules cannot diffuse into the cells but all mammalian cells have to be able to internalize extracellular substances. It is necessary since the cell must communicate with the external world; this includes the uptake of essential nutrients and the ability to have an effective defence against invading microorganisms. One of those mechanisms is called endocytosis and is used in PCI [12], [13]. In endocytosis, the cell membrane encapsulates the substance and takes it into the cell. In the cell, the substance is trapped in an endocytic vesicle. This process is used by the cell to take in large molecules that cannot pass the plasma membrane in another way. The substance will be delivered to the organelles or destroyed if it is not recognized. This mechanism can thus be used also to deliver drugs or therapeutic agents to the cytosol.

When the drug is inside the cell, encapsulated in the endocytic vesicles, it must be able to escape from those vesicles before it will be degraded. Many drugs cannot escape and have so far not been possible to deliver using this mechanism. PCI is short for Photo Chemical Internalization and is a method to deliver large molecules into the cytosol by disruption of the endocytic vesicles.

PCI uses the same principles as PDT, see section 3.1, but instead of killing the cell, only the membrane of the endocytic vesicles are to be destroyed. The goal is to localize a photosensitizer in the membrane of the endocytic vesicles. When the drug is activated by light of the right wavelength it will be excited. This energy can be transferred to oxygen and reactive species of oxygen will be formed. The most important reactive specie is singlet oxygen [2]. Singlet oxygen will react with what is nearby (20-100nm) and destroy the membrane of the vesicles [14]. The therapeutic agent is released to the cytosol and can reach the target. See figure 3.1.

The choice of photosensitizer is of ample importance. The photosensitizer must be able to enter into the cell and localize in the membrane of the endocytic vesicles. Some photosensitizers, such as $AlPcS_4$, cannot penetrate into the plasma membrane and will be taken up into the cell by other mechanisms than endocytosis. The photosensitizers that are interesting for PCI are those who can localize in, but not get through, the plasma membrane. They will be taken into the cell by endocytosis and thus end up in the membrane of the endocytic vesicles. Photosensitizers with an amphiphilic structure with a hydrophilic part are considered as the most efficient photosensitizers for PCI, [13].

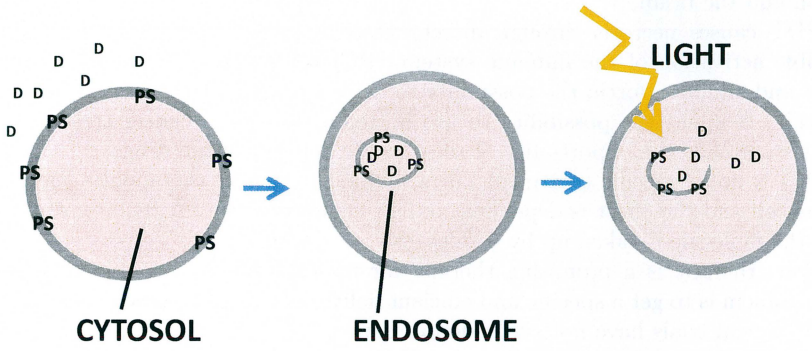

Figure 3.1: Schematic picture of the release of the content from an endosome. D is the drug to be delivered, PS stands for the photosensitizer.

3.3 Dosimetry

The outcome of the treatment is dependant of many parameters. The PCI effect is dependant of the amount of light that is given to the tissue but also the amount of oxygenation and the amount of photosensetizer present in the tissue. To be in control of the treatment, all parameters should be monitored to make it possible to adjust the light dose for the aimed outcome. The amount of photosensitizer given to the patient is controlled but how is the photosensitizer distributed in the body and within the area to be treated? A possibility is to monitor the fluorescence from the photosensitizer at many different locations in the area. Theoretically it is then possible to, through tomography, reconstruct the distribution. The singlet oxygen can be monitored through luminescence at 1270nm [2]. The problem is that the signal is weak due to the short lifetime of singlet oxygen. The most often used model for the dosimetry is to assume a fully oxygenated tissue and an even distributed concentration of the photosensitizer. Only the amount of light delivered to the tissue is monitored. Using the Spectra Cure system the fluence rate can be monitored by measuring the optical properties and then use a forward calculation as described in Chapter 2.

3.4 Possibilities for the PCI-technology

PDT is clinically approved for early stages of several cancer types and for palliative treatment of more advanced tumours. Despite this, PDT has not yet got its great break through. Several reasons are mentioned such as a lack of photosensitizer specificity and the lack of a reliable dosimetry in oncology [13]. The maximum tolerated light dose is often lower than the light dose needed

to treat the whole tumour, especially in sensitive regions as the head and neck region and the brain.

PDT causes necrosis through direct cytotoxic, vascular starvation and a possible activation of the immune system. PCI has shown to have the same effect and adding a forth: the possibility to deliver drugs to their targets inside the cell. It opens the possibility to use bigger molecules in cancer treatment and also provide the opportunity of site-specific delivery of the drugs.

PCI is not a specific treatment but a method to deliver therapeutic agents to the cell and the effect is dependent on the choice of agent. A requirement is that the molecule is taken up by endocytosis.

Gene therapy is a promising therapy for many diseases, not only cancer. The problem is to get a specific and efficient delivery of the macromolecules and many clinical trials have not succeeded as expected [15]. One example of gene therapy is siRNA (silencing RNA).

Bleomycin is a commonly used chemotherapeutic agent and it has been shown that its toxicity can be increased when used with PCI. The doses of Bleomycin can then be decreased and the negative side effects can be limited. Bleomycin is a small molecule compared to proteins and genes and this shows that the PCI-technique can also increase the uptake of smaller molecules. The treatment effect of the combination of PCI and Bleomycin is currently examined in a phase one study in London.

Chapter 4

SpectraCure's light delivery system

Spectra Cure has four hardware systems for delivering of light and for real-time monitoring of μ_{eff}, the photosensitizer fluorescence and the tissue oxygenation. The main idea of Spectra Cure's systems is the possibility to switch between two modes, the treatment mode and the measurement mode. In measurement mode, the effective attenuation coefficient, μ_{eff}, is evaluated and the result is used to adjust the treatment. This leads to the possibility of an individualized and real-time dosimetry.

The newest system is constructed to be used in PDT-treatment of prostate cancer and consists of 18 lasers coupled into 18 400 μm patient fibres. In the measurement mode, only one laser will irradiate while six patient fibres coupled to spectrometers will be used to measure the light at their positions. The number of fibres is chosen so that the entire prostate volume can be treated during a reasonable time. The wavelength of the lasers depends on the choice of photosensitizer since the wavelength must match the absorption spectra in the photosensitizer.

4.1 P1 - The system for the preclinical trials in Norway

In the preclinical trials in Norway, one of the prototypes has been used and the system will be referred to as P1. P1 uses the wavelength 652nm to match the photosensitizer developed by PCI Biotech AS. P1 has eight patient fibres and since the mouse tumours in the trial are small, three lasers are considered to be sufficient for treating the volume. The five remaining fibres are used for detection only.

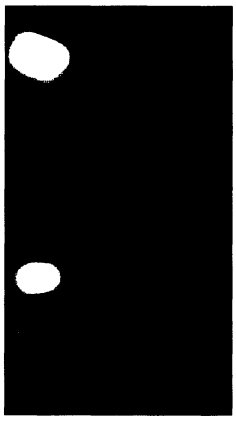

Figure 4.1: Picture from the spectrometer where two spots are saturated. The top spot risk leaking to the spot below.

4.1.1 Lasers

Three diode lasers at a wavelength of 652nm are used and they are mounted on a cooling plate to ensure a low and stable temperature. The output power of a diode laser is strongly dependant on the temperature. The output current from the laser drivers is decided by setting a value between 0 and 255. The same value does not give the same output power for all three lasers and calibration is needed. Since the cooling is external, the temperature in the laser diode is not precisely known and it is reasonable to think that a change in current to the laser will lead to a non-stable output just after the change. This can be a problem since the lasers will only irradiate for a short time during the measurement sequence.

4.1.2 Detector fibers and the CCD-camera

The five detector fibres are coupled to the same spectrometer but with different angles, resulting in five spots at different height. The spectrometer can be run with either eight or twelve pixels resolution. The value of each pixel with in an predefined area is summarized to obtain the total light from one fibre. When the fibre collects too much light, some pixels can be saturated and the size of the spot risks being too big, resulting in a leakage to the other spots at the detector. The detectors need to be calibrated since the same fluence rate will not give the same total light at the detector for every fibre.

Chapter 5

Development of PCI-dosimetry for preclinical trials on mice

My intention with this chapter is to give an introduction and an understanding for the different parts in the dosimetry planned to be developed for the pre-clinical and clinical study within the Eurostars project. Not all parts will be used in the preclinical study but are included for future needs. I will provide an overview to make it clear how they interact and how they affect each other. The different parts will be treated in detail in the next sections.

5.1 Overview of the dosimetry

The simulations and the discussions in this chapter are based on a simple, and not very realistic, model of a mouse. There are several reasons for this. One is that not much was known about the real situation when I started this project. Another reason is that using a simple and general model gives a better understanding for the problem. What is learned from the simple model can be applied in many situations, such as in the preclinical trials on mice but also in the future when the method is to be developed for human head and neck cancer. During the project I have had more input from the group in Norway and in the end of this chapter I will discuss which adaptations in the model, theory and practice that must be done in order to be able to use the dosimetry in the pre-clinical trials.

As mentioned in the section about dosimetry, the goal is to irradiate the tissue for a specific time to provide just the right amount of light to provide the PCI effect in the entire region of interest. This specific time should be calculated so that the tissue to be treated receives a light dose that is within a pre-determined interval suitable for PCI. In the flowchart in figure 5.1 the steps

from a desired light interval in the tumour to irradiation times for each fibre are depicted. The ovals represent the decisions that must be taken and the arrows show which steps that are dependant of those decisions.

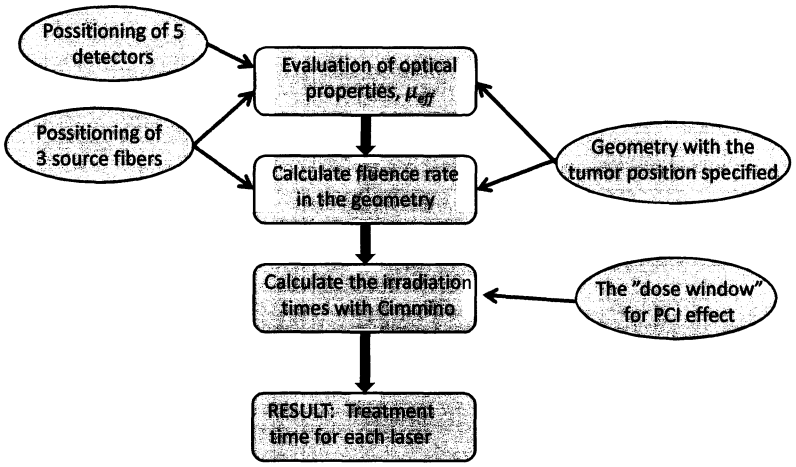

Figure 5.1: Overview of the different parts in the dosimetry

In order to know the fluence rate in the whole geometry the optical properties of the tissue must be evaluated. The fluence rate is measured at fifteen different distances and the experimental values are fitted to the theoretical curve from the analytic model, see equation (2.2.9) in Chapter 2, with a non linear fit and μ_{eff} can then be retrieved. This step is dependent of both the positions of the source fibres and the positions of the detector fibres. The fibre positions are important since the combination of source and detector positions must give distances that are well spread out in an interval, see section about evaluating μ_{eff} in Chapter 2. The evaluation of μ_{eff} is also dependant on the geometry because the geometry will decide which analytic model that is to be used. If a more complicated model is used it is not possible to describe the light propagation with an analytic function and FEM or Monte Carlo simulations must be used instead.

When the optical properties and the positions of the source fibres are known, the fluence rate can be calculated using, for the simple geometry, the analytic function. The last step is to find the irradiation time for each source fibre. In order to find the times, the Cimmino algorithm [16] can be used or they can be estimated directly in simple cases. The algorithm takes the fluence rate and the

geometry as inputs and calculates the time each fibre must irradiate in order to achieve the desired light dose throughout the entire treated volume. To solve the problem, a system of linear inequalities has to be solved. In the Cimmino algorithm, different weights can be assigned to the inequalities. The weight corresponds to how important it is to deliver a light dose that is exact within the pre-defined interval. For sensitive organs, the weight is high but the weight will be lower for normal tissue.

The position of the source fibres decides if it is possible for the Cimmino algorithm to find a solution; it is not certain that a given position of the source fibres can deliver a light dose in the whole tumour that is within the desired interval.

When developing the dosimetry for PCI-treatment, all the parts mentioned previously must be considered. The positioning of the detectors and the sources affect how well the optical properties can be evaluated but the positions of the sources also affect the possibility for the Cimmino algorithm to find a reasonable solution. I will discuss different possible solutions and also discuss the trade-offs that must be done. The solutions will differ if it is for a dosimetry in a pre-clinical trial on mice or if it is, for example, a treatment of cancer in the head-neck region of a human. I will mainly focus on the dosimetry that will be used in the pre-clinical trials within the Eurostars project, but some of the discussion and conclusions will be general for dosimetry in PCI treatments.

5.2 Geometry

The model used is a half infinite cuboid and the tumour is modelled as a half sphere, see figure 5.2. The choice of a simple model allows an analytic treatment of light propagation and the geometry can easily be emulated by means of phantoms.

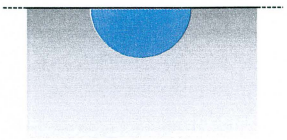

Figure 5.2: Simple geometry

5.3 Threshold dose model

As described before, the most commonly used dosimetry model relies on the three components involved; fluence rate, concentration of photosensitizer and tissue oxygenation. It is not evident how to achieve those components, and often it is just the fluence rate that is measured, while values for the other two are assumed. The dosimetry in the mouse study will be based on the fluence dose [2]:

$$D_{flu}(\mathbf{r}) = \int \phi_x(\mathbf{r}, t)dt \tag{5.3.1}$$

When the dose that gives the desired effect is reached, the treatment will be stopped. This is called the threshold dose. It is worth to notice that this model assumes a fully oxygenated tissue and an even distribution of the photosensitizer.

It is evident that the choice of threshold dose is important for the outcome of a treatment. PCI biotech has already done studies on mice where they used a

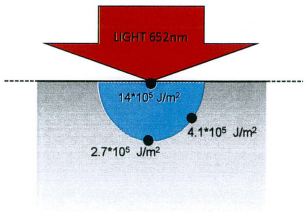

Figure 5.3: Fluence dose at different positions in the tumour

laser diode emitting at 650nm. The irradiance was 50mW/cm^2 and the spot had a diameter of 8mm and the treatment time was between 300 and 400s. Through biopsy it could be established that the PCI effect was seen in the entire tumour. By knowing this it is possible to ascertain the light dose given in the different parts of the tumour (the tumour is expected to be a half sphere with radii 3mm). A Monte Carlo simulation was performed for a pencil beam on a thick slab. The result was convolved in order to simulate the light spot used in Norway. For the resulting doses, see figure 5.3.

If the dose is high, there can be a PDT-effect as well. When evaluation the PCI-effect it is not desired since it will kill the cells and the result of the PCI-treatment will be destroyed. What is described above is a basic first try and later studies have shown that the situation is more complicated. The ongoing preclinical trials indicate that the threshold dose for PDT with the photosensitizer Amfinex differs between different parts of the tumour. It seems like the edge of the tumour is less sensitive than the centre. The trials will continue and will try to establish if this is the case also for PCI with bleomycin and siRNA.

5.4 Fiber positioning

The system to be used in the preclinical trials is described in Chapter 4 and uses three fibres to deliver light and five detector fibres to evaluate the optical properties in the tissue. In the trials, the goal is to deliver a smooth light dose in the tumour in order to have the PCI effect but not the PDT effect as described in section 3.3. It is also important to be able to deliver the light dose in a reasonable short time. Those aspects are of importance when deciding where to place the source fibres. During the treatment, the optical properties will be evaluated and this evaluation will be better if the distances between the source fibres and the detection fibres are well spread out in an interval of approximately 5 to 20mm. The fibres can be placed either on the surface or interstitially. The pros and cons for the different ways will be discussed.

5.4.1 Source fibers

The first question is whether the fibres should be placed on the surface or interstitially. Interstitially, the light can be delivered from different sides of the tumour and this will lead to a smaller gradient of the fluence within the tumour as compared to if they were placed within the tumour region. If the interval between the low and the high threshold dose is tight this might be the only way to achieve the necessary dose in the tumour. With the lower and upper threshold dose indicated in section 3.3 it is possible to achieve the desired dose in the entire tumour even if the fibres are placed at the surface. During a treatment, interstitially placed fibres can cause blood pooling at the fibre tips and complicate the dosimetry. The result of the discussion is that the fibres will be placed at the surface.

Other advantages of surface illumination are that the mice are small and it

is complicated to place fibres at the desired positions interstitially, and it would be complicated and painful to use interstitial fibres. When using the method on humans, it will be necessary to use interstitial fibres for some tumours.

The fibres are placed in the corners of a triangle over the tumour. The distance to the centre is changed in the simulations. By positioning the fibres longer from the tumour, a smoother light dose distribution can be achieved, but the irradiation times will be longer.

The difference in smoothness, depending on how far the fibres are placed from each other, is of interest. As an example two different source positions were compared, one where the distance to the centre of the tumour is 6 mm and one with 9 mm distance. The calculations where done using the diffusion approximation, see equation (2.2.6), assuming an infinite medium. It is the ratio between the fluence rate at the point the farthest away and the closest point that are interesting and this number should be as low as possible. I compared the ratio for the two different source positions and found that the ratio is 1.7 times higher for the closest source position. This is expected since a factor of r^{-1} is present in the diffusion equation.

5.4.2 Detector fibres

The detector fibres will be placed at the surface of the mouse. By using three source fibres and five detector fibres, each detector fibre will measure the light from three lasers. The result is fifteen measurements of the light at different distances from a source which will be available when calculating the optical properties. The positioning should be such that the fifteen distances are spread out between approximately five and fifteen millimetres. It is possible that the optical properties differ between normal tissue and tumour tissue. It is therefore desirable to place the detector at the opposite side of the tumour compared to the source so that the photons mostly will pass through the tumour. Probing through the tumour is hard to realize for small source-detector distances and one solution can be to place one detector fibre on top of the tumour.

5.5 Evaluation of μ_{eff}

To evaluate μ_{eff} the inverse problem must be solved. The experimental data is fitted to data from the forward model through minimization. The forward model is discussed in section 2.2 in Chapter 2 and since the geometry is half infinite, an analytic solution to the diffusion equation, equation (2.2.9), can be used. It is also possible to use an expression for the diffuse reflectance out of the boundary and the equation is given in (2.2.10). The value of z_b is important and can be retrieved using the equations given in (2.2.8) and [4] if the refractive index of both materials are known. It is the difference between the normalized fluence rates from the forward model and the normalized experimental values that is to be minimized. The normalization is due to that the light measured is proportional to the fluence rate.

Either it is the absolute error that is minimized or the relative error. If the absolute error is used the fit will be based on high values, which implies short distances. Therefore it is a better solution to minimize the relative error. For minimization the Matlab function **lsqnonlin** is used. lsqnonlin uses either the 'trust-region-reflective' or the 'levenberg-marquardt' algorithm.

5.5.1 Evaluation of μ_{eff} from simulated data

The method to evaluate μ_{eff} must be validated through experiments and simulations. A first step is to simulate measurements using COMSOL where source positions, detector positions and optical properties are set. The simulated data is fitted to the theoretical curve as if it was experimental data, and μ_{eff} is retrieved. μ_{eff} is expected to be close to the μ_{eff} set in COMSOL.

μ_a is set to 50 m^{-1} and μ_s' to 900 m^{-1} in COMSOL. The result from the evaluation is seen in table 5.1. The evaluation is performed with two different theoretical models as described in Chapter 2. It is either the absolute error or the relative error that is minimized. Table a) shows the results when all data points are used in the evaluation, meaning all source-detector distances. Table b) shows the results when only data points with a source-detector distance greater than 5mm are used.

(a)

	Minimizing absolute error	Minimizing relative error
Diffuse reflectance	42.9	56.9
Fluence	73	58.5

(b)

	Minimizing absolute error	Minimizing relative error
Diffuse reflectance	62.9	60.0
Fluence	56.5	53.5

Table 5.1: Evaluated μ_a in m^{-1} from COMSOL generated measurements using different theoretical models. Source-detector distance ranging from a) 2 to 12 mm. b) 5 to 12 mm

The result shows big differences between the different models, the different data points used and which error that is used in the minimization. Using the direct error makes the fit mainly adjust to the measurements at short distances. The result is that measurement errors or model errors in those data points will have a big impact on the result. Generally a better result is obtained when minimizing the relative error. The results are in general higher than the expected μ_a=50m^{-1}. The analytic model and the FEM-simulations use different ways of modelling the boundary. It is a possible explanation of the non-coherent results. By using the fluence rate model and source-detector distances greater than 5mm the best result is achieved in this case.

5.6 Dosimetry for a more realistic mouse model

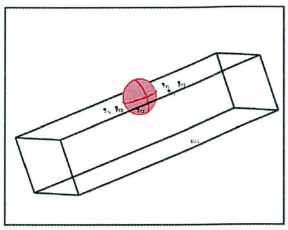

Figure 5.4: A slightly more realistic model of a mouse leg

After visiting the group in Norway a more realistic model was created. The model used is a cuboid measuring 10x20x40 mm with a spherical tumour of size 3-7 mm in diameter. See figure 5.4. A question is now whether the change in geometry affect the previous discussion concerning fibre positions and evaluation of μ_a.

The positioning of the fibres is limited by the geometry of the mice. The practical details will be discussed in Chapter 7. The change in geometry can have great impact on the evaluation of μ_{eff}. The analytical forward model used in the inverse problem does not fulfill the geometry assumptions. A numerical method or a Monte Carlo simulation can be used as the forward model, see Chapter 2. It is also possible to use the analytical model for a semi-infinite geometry as the forward model but the result will be more or less accurate.

5.6.1 Using the analytical half infinite forward model

Even if the analytical model for light propagation is not fully valid it is still possible that the resulting μ_{eff} is acceptable. Three models were built up in COMSOL and the resulting fluence rate was used to evaluate the μ_{eff} using the analytical half infinite fluence model as the forward model. The result can be seen in table 5.2.

Geometry in COMSOL	μ_a
Half infinite	58.5
Cuboid 10x20x40mm	59.1
Cuboid with tumour 3mm	56.8
Cuboid with tumour 6mm	49.7

Table 5.2: μ_{eff} is evaluated for different geometries by fitting data from COMSOL with the semi-infinite analytical model

The estimated μ_a is higher for the cuboid than for the half infinite geometry. It is expected since less light will penetrate to the detectors far away due to boundary losses. When introducing a tumour in the cuboid the estimated μ_a increases with tumour size. More light will penetrate to detectors at long distances due to the increasing distance to the boundary. Using the half infinite analytical solution as the forward model in the inverse problem result in an underestimation (compared to the half infinite case) of μ_a of about 18 % for a tumour size of 6mm in diameter.

5.6.2 FEM-simulations as the forward model in the inverse problem

Using a FEM-simulation as the forward model allows an arbitrary geometry. The FEM-simulation is based on the diffusion equation, and the constraints of

the diffusion approximation must still be taken into account. By using computer software, FEM-simulations can be integrated in Matlab. Nirfast is an FEM based package for modelling near-infrared light transport in tissue [17].

Chapter 6

Experimental

In Chapter 5, different parameters affecting the evaluation of μ_{eff} were discussed and simulations were performed in order to estimate how well μ_a could be estimated if μ_s' was considered known. The simulations and discussions need to be justified through experiments. The experiments are performed using tissue phantoms. The experiments will also contribute to a better understanding for the system and its limitations and the scripts written for calibration, measurements and evaluation will be used in the preclinical study in Norway. In the end of this chapter, it is discussed which conclusions that can be drawn from the measurements and how the measurements can be improved.

6.1 Materials and method

The P1-system with five detector fibers and three source fibres will be used for the measurements. For more details see Chapter 4. The fibres will be placed at the surface of the phantom, fixed through holes in a black delrin plate.

6.1.1 Measurements

The three source fibres will be turned on one by one and the five detector fibres will register the amount of light. All detector fibres are connected to the same spectrometer and the same CCD-detector. For the measurements, the CCD-detector is used in a mode that provides an 8 bit intensity resolution. The light from the five detector fibres is directed in different angles, hitting the detector at different heights, see figure 4.1 in Chapter 4. The shutter time can be changed and needs to be adjusted in order not to saturate the detector and to have a sufficiently high signal. Since the shutter time should be optimal for all the five measurements, three pictures with different shutter times are taken for every measurement.

6.1.2 The phantoms

In the experiments the optical properties of the phantoms should be similar to those of mouse tissue. The optical properties for different mouse tissue can be found in an article by Alexandrakis et al. [18]. It is important to note that those values are not exact values, but they can be used as a guide-line. In the animal study, the tumour treated will be localized at the hip of the mice. Relevant optical properties are for skin and muscle. By using the formulae given in the article, the optical properties are as follow:

$$\mu_{a\_muscle} = 0.61\text{cm}^{-1} \qquad \mu'_{s\_muscle} = 4.6\text{cm}^{-1} \tag{6.1.1}$$

$$\mu_{a\_skin} = 0.65\text{cm}^{-1} \qquad \mu'_{s\_skin} = 23\text{cm}^{-1} \tag{6.1.2}$$

The phantom is a liquid made of intralipid and ink. The intralipid consists of small fat particles and has scattering properties similar to those of tissue. The ink is used for increasing the absorption of the phantom. Water and 10%-intralipid are mixed together and the solution is divided between four containers and different amount of ink is added. In order to know the exact scattering and absorption of the phantoms, measurements were performed with a time-of-flight system (TOF-system) as described in Chapter 2.

Phantom nr.	ink (ml)	μ'_s (cm^{-1})	μ_a (cm^{-1})
1	3	9.10	0.29
2	5	9.00	0.48
3	7	9.15	0.65
4	9	9.10	0.82

Table 6.1: Optical properties of four phantoms measured with the TOF-system

The fit between the measurements and the theoretical curve is good. The scattering should not differ much between the phantoms and the result shows that it does not. Those two indications make the TOF-results reliable.

6.1.3 Boundary conditions

The eight fibres are placed through holes in a black plate made of delrin with a refractive index of 1.48. The plate is in contact with the phantom during the measurements. The fibres are placed either at the surface of the phantom or 2-3mm down in the phantom. The plate prevents reflections from the surroundings. The parameter z_b decides where the imaginary source is placed, see 2.3, and is calculated from the equations given in [4]. For a boundary between intralipid phantom (n $\approx$ 1.4) and delrine plate (n $\approx$ 1.48) $z_b \approx$ 0.8mm.

6.1.4 Experiments

The experiments are performed using two different ways of positioning the fibres. The first set of fibre positions results in source-detector distances ranging between 4 and 15mm and the second set of fibre positions results in distances between 10 and 25mm. Vertically, the fibres are placed either just at the surface of the phantom or at a depth of some mm. All measurements are done with both sets of fibre positions and with the two different vertical positions. Each measurement is repeated three times. Measurements are performed on the four different phantoms mentioned above.

6.2 Results

As described in section 5.5, μ_{eff} can be evaluated using different light propagation models. The analytical solution for the half infinite geometry of the diffusion approximation is used for evaluating the absorption coefficient for the phantoms. When the fibres are positioned some mm down in the phantoms, the forward model used is the equation for the fluence rate. If the fibres are placed at the surface of the phantom both the expression for the fluence rate and for the diffuse reflectance are tested as the forward model. In all graphs, the time of flight measurements (TOF) are shown as a reference.

6.2.1 Fiber positions with 5-15mm source detector distances

In figure 6.1 the result for the evaluation of μ_a is shown. When the fibres are placed some mm down in the phantom, the result does not differ more than 6% from the TOF-measurements, see figure 6.1(a). For measurements where the fibres are placed at the surface, the result depends on which model is used for the evaluation. In figure 6.1(b) the fluence rate is used and in 6.1(c) the diffuse reflectance is used. The conformance with the TOF-results is clearly better in 6.1(c).

6.2.2 Fibre positions with 10-25mm source detector distances

In figure 6.2 the result for the evaluation of μ_a is shown. When the fibres are placed some mm down in the phantom, the fluence rate model is used. For measurements where the fibres are placed at the surface, the diffuse reflectance model is used. In figure 6.2(a) all source-detector distances are used in the evaluation but in 6.2(b) only source-detector distances resulting in relative fluence rate above 5% of the mean fluence rate are used. The result in 6.2(b) is considerably better than the result in 6.2(a).

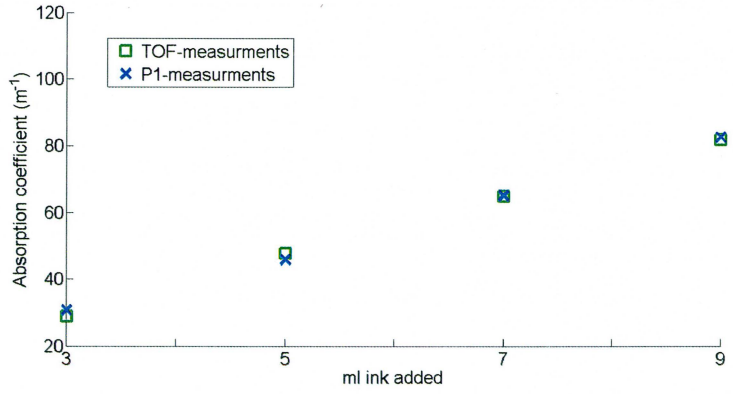

(a)

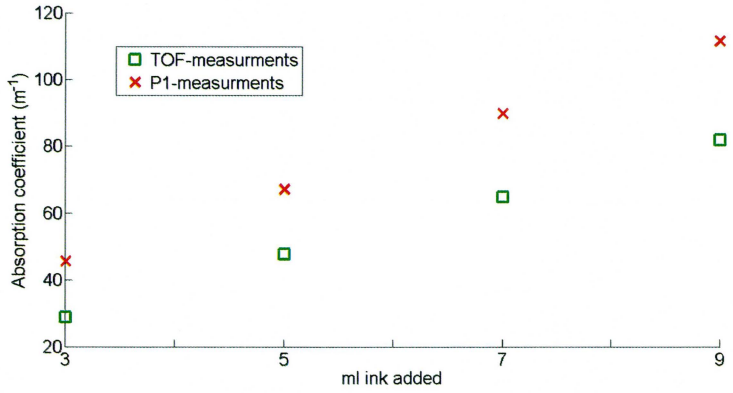

(b)

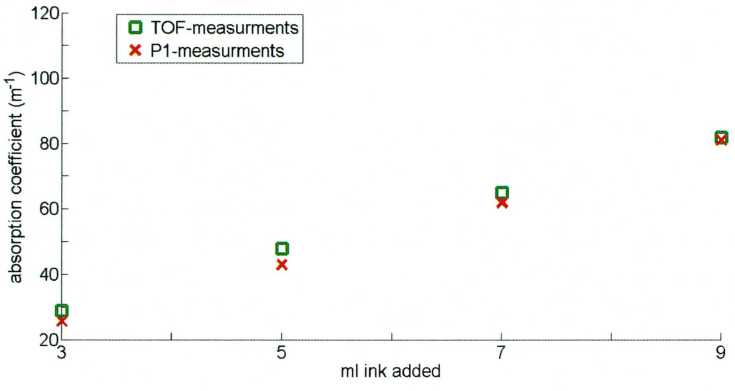

(c)

Figure 6.1: The evaluated μ_a for source-detector distances 5-15mm. Blue crosses: Fibres 3mm down in phantom. Red plus-sign: Fibres at the surface. a) Fibres placed 3mm down in the phantom. Evaluation with fluence rate. b) Evaluated with fluence rate. c) Evaluated with diffuse reflectance.

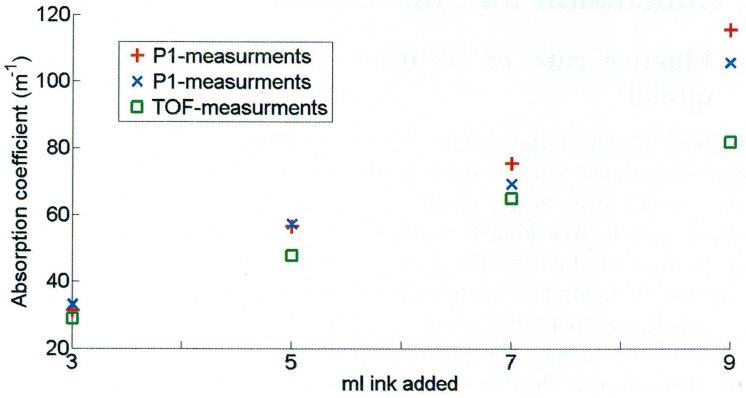

(a)

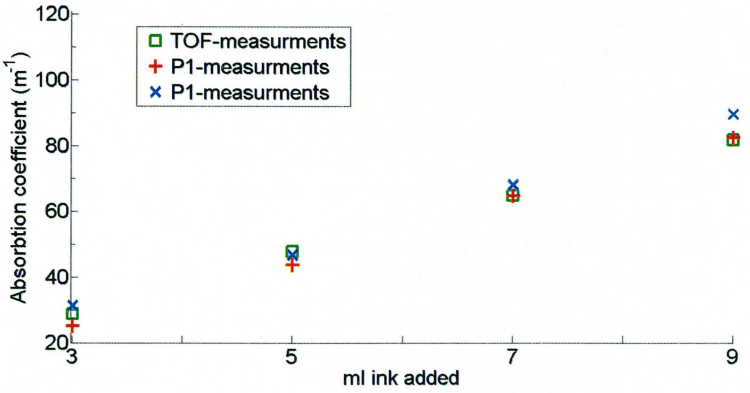

(b)

Figure 6.2: The evaluated μ_a for source-detector distances 10-25mm. Blue crosses: Fibres 3mm down in phantom. Red plus-sign: Fibres at the surface. a) All source-detector distances. b) Source-detector distances $\approx$ 10-17mm

6.3 Conclusion and discussion

6.3.1 Fluence rate or diffuse reflectance as the forward model

For the fibres placed at the surface of the phantom either the fluence rate or the diffuse reflectance can be used as the forward model. Using the diffuse reflectance model gives better results as can be seen in figure 6.1. Using the fluence rate model gives higher μ_a than expected. It implies that the curve showing the relative fluence rate as a function of distance are steeper for the measurements than for the fluence rate model. When fitting the theoretical curve to the measurements the result is a higher μ_a.

An explanation to why the fluence rate model does not work for measurements at the surface is that we do not measure something proportional to the fluence rate but something proportional to the change of the fluence rate in the z-direction. The gradient in the z-direction is greater for shorter distances than for longer, explaining why the value for shorter distances is higher than expected in the fluence model. In the diffuse reflectance model, it is the gradient of the fluence rate that is described and more accurate values are achieved. It is also possible to combine the fluence rate and the diffuse reflectance to achieve a model that is more accurate [19]. For the measurements recorded inside the phantom, the fluence rate can be used since the gradient of the fluence rate is proportional to the fluence even if the distance from the source changes.

6.3.2 Why are the result more inaccurate when using longer source-detector separations?

In subfigure a) in 6.2 it is clear that the result for longer source-detector positions is inaccurate. In subfigure b) in 6.2 only data from shorter source-detector distances are used in the evaluation and the result is greatly improved. The reason is that the signal is too low for the longer source-detector distances and the resulting light captured at the detector is too low to give an accurate result. The lsq-algorithm will fit the theoretical curve to noisy or erroneous data resulting in inaccurate absorption coefficients. During the measurements three fixed shutter times were used. For long source-detector distances and high absorption the longest default time was insufficient. The shutter times must be better adjusted in order to have good results at longer distances. A problem is that a long shutter distance can result in a leakage from a saturated neighbour detector.

6.3.3 Possible improvements of the measurements and the evaluation

To improve the measurement, a higher resolution should be used. Using more bits gives the possibility to measure the light near the source as well as the light further away from the source. The three exposure times should be chosen

more carefully and if needed, more than three exposure times can be used. For long distances, the problem with leakage from nearby saturated spots can be solved by using individual detectors for all fibres. This requires a major change of the hardware. The results show that using the diffuse reflectance model as the forward model in the evaluation gives good conformance with the time of flight measurements. To improve the results even further, a Monte Carlo model can be used as the forward model. To improve the analytical model, the diffuse reflectance model and the fluence rate model can be combined as mentioned in [19].

Chapter 7

Preclinical trials in Norway

The Eurostars project is divided into seven work packages (WP's). In WP1 and WP2 *in vitro* experiments are performed to establish the most efficient deliver vehicle and to screen for siRNA that has an anti-cancer activity. Those work packages are performed by siRNA Sense and PCIBiotech. In the third WP the goal is to establish conditions for PCI *in vivo* where the content of the endosomes can be released without significant toxicity in the tumor and the normal cells at the border of the tumor. Spectra Cure's contribution is to provide the illumination device and to help with the dose evaluation when looking at the treatment results.

The experiments performed in Norway are described in the first section of this chapter. The following sections are devoted to an evaluation of the μ_{eff} for the mice, the result of the treatment and the delivered light doses. The experiments have just started and the results that are presented here are to be considered as preliminary due to the small number of tumors treated. The discussion is focused on the first conclusions that can be drawn and, more important, on the development and improvements that are to be done.

7.1 Experiment

The *in vivo* experiments are performed on mice at Radium hospital in Oslo, Norway. Spectra Cure's system was used for the first time in the end of November on five tumors. It was mainly a test to see if the probes manufactured for the trials worked satisfactory and to discuss the treatment and the user interface of the program that controls the lasers.

For the first session of experiments, the times are decided before the experiments. There is no feedback from the measurements to the treatment times and variations of the tumor size are not taken into account. In later experiment sessions, those aspects will be taken into account. The measurements are performed with the goal to collect data and through post evaluation understand how the data is best evaluated.

Figure 7.1: Picture taken with the IVIS-system

7.1.1 Material and method

The mice with tumors

The mice have a tumor on the hip, in some cases on both hips. The tumor cells are altered to carry the firefly gene containing luciferase. Luciferine is injected into the blood and react with the luciferase and photons are emitted in the reaction. The photons are detected on a sensitive CCD-camera using a commercial system called IVIS. The reaction can only take place in parts of the tumor supplied with blood. An example of a picture from the IVIS-system can be seen in figure 7.1

The probes

The positioning of the detector and source fibers are decided in Chapter 3.3. Four probes were designed and manufactured for the preclinical trials. The challenge is to construct a probe that can maintain contact between the fibers and the skin of the mouse.

Spectra Cure system - P1

The system referred to as P1 is used during the clinical trials and is described more in detail in Chapter 4. The lasers operate at approximately 30mW but one laser was not stable in output power and was changed for the next treatment session. The stability problem does not affect the treatment but is a problem for the measurements. The camera has 12 bits effective resolution. The measurements are done with three different exposure times, 5, 100 and 500 ms.

7.1.2 Finding realistic illumination times for point source light delivery

Before Spectra Cure's system was used, the group in Norway used surface illumination. 5, 10 or 20J/cm^2 was delivered to the surface of the tumor. For the first treatment session using the Spectra Cure system, the irradiation time should be so that the light dose is comparable to the case of surface illumination. A Monte Carlo simulation of the surface illumination was performed and the resulting light dose in the middle of the tumor was 130J/cm^2. The geometry used is a slab with thickness 2cm and is not a realistic model. For the case with three point sources (Spectra Cure system), a FEM-simulation was performed on a realistic geometry. The fluence rate in the middle of the tumor was $136*10^{-4}$J*s^{-1}cm^{-2}. The irradiation time of each laser is set to approximately 350s in order to deliver the corresponding light dose with three fibers as was delivered using surface illumination.

When using surface illumination, the group in Norway did not take the variation of tumor size into account. For a small tumor, the skin spot irradiated of the mouse was relatively small and vice versa for a big tumor. The J/cm^2 was constant but the total energy delivered was not. The method to decide the

corresponding illumination times for three lasers is coarse, since an unrealistic Monte Carlo model is used, but this is not of great importance at a first stage.

When illumination times are found that result in the desired effect in the tumor, a more exact evaluation of the light dose will be performed. Since the geometry is small, the best forward model is the Monte Carlo model. A Monte Carlo model for a more mouse leg like geometry is under development.

7.2 Evaluation of μ_{eff}

The measurements are performed with three lasers and five detector fibers, resulting in fifteen data points. In the evaluation of the first session in Norway, only ten data points were used because of the power fluctuations in one laser. The μ_{eff} searched for is the μ_{eff} resulting in the best fit between the forward model and the data points. At a first stage, the forward model used is the analytical half infinite forward model. In the continuation of the project, a more realistic model will be developed.

7.2.1 Result

It was a problem to maintain good contact between the fibers and the mouse. One of the mice was put to sleep during the measurement and this measurement is used for the first evaluation of μ_{eff}. The result of three other measurements are also shown. In the following treatment sessions, the mice will be put to sleep during the treatment and the measurement which will simplify maintaining contact between the mouse and the probe.

To evaluate μ_a, z_b and μ_s' must be set. μ_s' is set to 0.46 mm^{-1} according to table 6.1.1 in Chapter 6. z_b is given in equation (2.2.8) in Chapter 2 and if μ_s' = 0.46 mm^{-1} is used, the resulting z_b is 4.3 mm.

Using the parameters above, the result from four measurements on mice is shown in table 7.1. The expected absorption coefficient is μ_a = 0.061 mm^{-1} accoring to tablel 6.1.1 in Chapter 6 and [18].

Mouse nbr.	μ_a (mm^{-1})
1 (put to sleep)	0.054
2	0.061
3	0.069
4	0.077

Table 7.1: Absorption coefficient of mice measured with the P1-system

During measurements on mouse 2-4, the mice moved and it was difficult maintaining contact between the fibers and the mouse. The fit between the measurement data and the theoretical curve for mouse 1 is seen in figure 7.2.

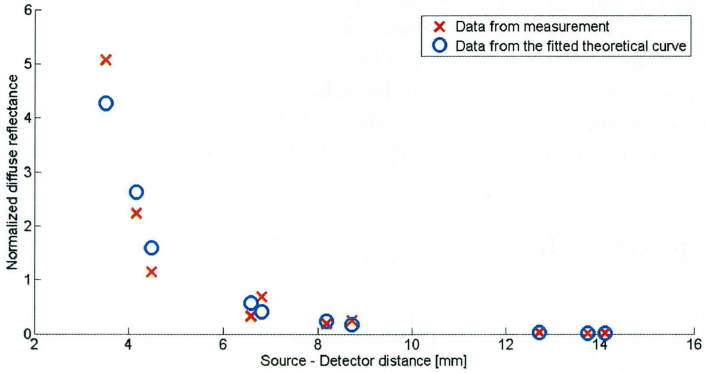

Figure 7.2: Fit between the measurement data and the theoretical curve

7.3 Evaluating the treatment effect

The first experiments were accomplished with a photosensitizer (Amphinex) but without an extra drug as siRNA or Bleomycin. It means that it is not the PCI effect that is examined but the PDT effect arising from the PCI specialized photosensitizer Amphinex. When Bleomycin or siRNA is added, the light dose needed to cause necrosis is expected to be significant lower. Up to date, only two mice have been treated with PCI with Bleomycin and much too little information exists to evaluate the result. The goal is to find the highest dose where no PDT effect is present.

To evaluate the treatment, pictures are taken of the tumor day -1 to day 3 relative to the treatment. Pictures are taken with a system called IVIS. The system detects the luminiscense that arises when the injected luciferin reacts with the altered tumor cells. The software chooses the region of interest (ROI) were the luminescence is over 5% of the maximum value in the picture. The pixel values are integrated over the region and a value, referred to as the ROI-value, is presented.

More experiments are needed to draw a conclusion of the results but many tumors follow the trend presented in figure 7.3. The treatment is performed day 0 after the picture is taken. The ROI goes down at day 1 and then starts to go up again. This is an effect seen in a about half of the pictures. The effect is likely from a shutdown of the blood vessels due to the PDT-effect.

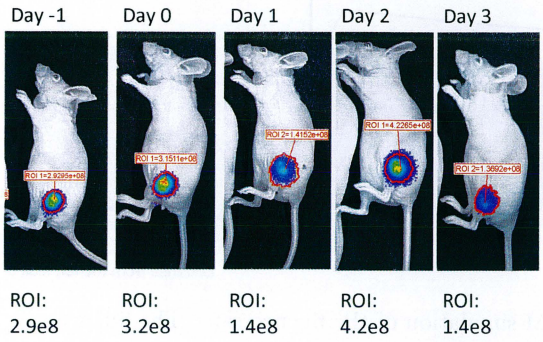

Figure 7.3: Development of the ROI from day -1 to day 3 relative to treatment

7.4 Light dose delivered to the tumor

It is interesting to know which light dose that has been delivered to the tumor during the treatment. Simulations are performed in COMSOL and the geometry used is a cuboid with a spherical tumor. The optical properties used are those from the article by Alexandrakis et al [18]. The fluence rate is plotted for two different lines through the tumor. The result is shown in figure 7.4 and 7.5. To have the light dose, the fluence rate is multiplied with the treatment length in seconds. As an example, the fluence rate in the center of the tumor is 1500 $\mathrm{Jm^{-2}s^{-1}}$. If the treatment time is 300s the resulting light dose is $5.5 * 10^5 \mathrm{Jm^{-2}}$.

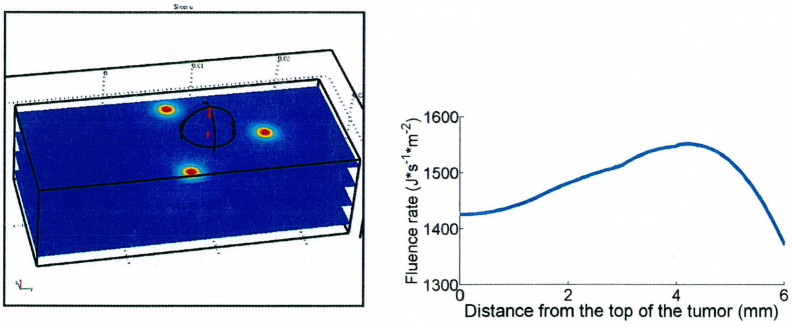

Figure 7.4: FEM-simulation of the fluence rate. The fluence rate along the red line is shown in the graph

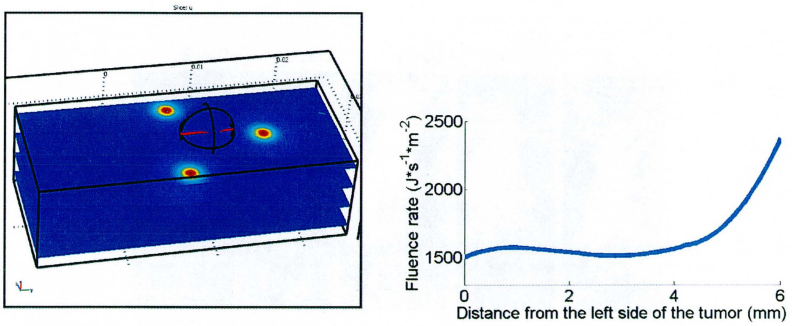

Figure 7.5: FEM-simulation of the fluence rate. The fluence rate along the red line is shown in the graph

7.5 Discussion

The long term goal with the pre-clinical trials in Norway is to establish optimal conditions for PCI-induced endosomal release in animal tumor models. The light dose needed for PCI is hopefully lower than the dose needed for PDT and a successful PCI-treatment with siRNA can treat the vicinity of the tumor without harming surrounding tissue. This is a big problem for PDT treatments. Too few experiments have been performed to draw conclusions about the light doses needed for PDT and PCI from the results. The discussion will therefore mainly focus on how to evaluate the data and which experiences that are gained from those first trials.

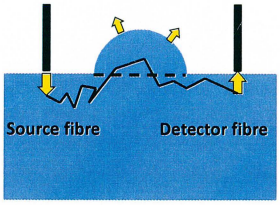

Figure 7.6: With out the tumour, the photons that cross the dashed line would not have the possibility to be scattered back and reach a detector. Photons reaching a detector far away from the source are more likley to have passed through the tumour. In the presens of a tumour, the fibre far from the source will measure an higher increase in intensity relative to the fiber close to the source.

7.5.1 Evaluation of μ_{eff}

The model used when evaluating μ_{eff} from the measurements is a rough simplification and the result is expected to be reasonable but not correct. From the simulations in Chapter 5, the error introduced by using an erroneous model is about 20%. The error is dependant of the tumor size, the size and form of the mouse leg and the fiber positions.

The result is close, closer than expected considering the assumptions made, to the optical properties presented in the article by Allexandrias et Al. [18]. As mentioned in Chapter 5, measuring on a cuboid result in higher μ_a due to higher losses at long distances. When introducing a tumor in the model, the losses for long distances decrease since the distance to the boundary increases when the photons pass through the tumor. This lead to a lower μ_a. To sum up, two main model assumptions are obviously not valid: Instead of an infinite geometry the leg is more like a cuboid and the surface is not flat because of a tumor that is shaped like a half sphere. See figure 7.6. The result is an over estimation respectively an under estimation of μ_a. In the simulations in Chapter 5 the result is an underestimation of μ_a. The mouse leg is even smaller than the cuboid in the simulations and this contributes to a higher μ_a. It is possible

that the two effects even out. The optical properties calculated from the article mentioned before cannot be taken as an absolute reference.

Improvements

To measure optical properties is difficult, and measure optical properties on mice is even more difficult because of the small geometry, the fact that they are moving and that they are strongly inhomogeneous. Some possible improvements will be mentioned here, but most of them are meant to be taken into consideration when proceeding to human clinical trials.

If the optical properties are to be evaluated with more accuracy, a realistic model of the mouse leg and the tumor must be used. A general model can be used, or a individual model can be created for each mouse. It is also possible to use a standard geometry for the leg but adjust the tumor size and position for every mouse. The fiber positions must be known. Since the geometry will be small, a Monte Carlo evaluation is interesting. There is a need for development of Monte Carlo models for divers geometries. When proceeding to clinical trials on head and neck cancer or pancreas cancer it is of more interest to develop an evaluation of the optical properties based on a FEM-model.

To be able to measure the light for a bigger span of source-detector distances, the leakage between two neighbor spots at the detector must be considered. The problem is solved by having individual spectrometers for the detector fibers or by positioning the detector fibers so the problem is avoided. The measurements can be improved if the lasers are more stable at start-up.

It is μ_{eff} that is evaluated when using typ spatial resolved measurement. To get μ_a right, μ_s' must be known. The relation between μ_a, μ_s' and μ_{eff} is given in equation (2.2.7). μ_s' has been taken from reference [18] but it could be of interest to measure the optical properties using a TOF-system.

7.5.2 Evaluating the treatment results

The region of interest is a 2D-picture of the surface of the tumor. The light that exits the tumor has been generated somewhere inside the tumor and then scattered. This makes it hard to extract the information of interest from the pictures. The total amount of light exiting the surface can be considered as proportional to the light generated as long as the tumor geometry does not change.

To improve the evaluation, it would be of great value to take pictures from different angles providing the opportunity to do tomography. It requires a change of the IVIS system which is not reasonable for the ongoing trials.

The evaluation will be easier if the mice are placed in the same position for every picture. It is also possible to follow the mice for longer time, then being able to follow the change of the tumor size.

Chapter 8

Conclusion and outlook

The goal of the master thesis was to develop a dosimetry and a concept for the PCI pre-clinical study on mice in Norway. The existing P1-system was modified to be used for the pre-clinical trials. Three fibres to deliver light were considered enough and the remaining five fibres were coupled to a detector. Simulations were preformed to better understand where to place the fibres in order to be able to at the same time measure the optical properties and deliver a smooth light dose throughout the tumour.

Before using the system in the pre-clinical trials in Norway it was tested on tissue phantoms in Lund. Scripts were written to control the P1 and to evaluate the optical properties of the phantoms. In the evaluation, a semi-infinite model was used. The optical properties of the phantoms could be evaluated with surprisingly good accuracy which was promising for the future measurements on mice.

In the preparation for the pre-clinical trials, probes were manufactured to maintain good contact between the fibre tips and the skin of the mouse. The group in Norway had already treated some mice using one laser illuminating from a distance and simulations were performed to find the irradiation times giving about the same light dose in the tumour.

During the pre-clinical trials on mice, some difficulties were encountered. The mice were smaller than we had foreseen and the tumours were varying strongly in position and in size. During the treatment, the mice moved and it was hard to maintain contact between the fibres and the mouse. The semi-infinite geometry model was used for the evaluation as planned, but the consistence between the model and the reality was worse than expected due to the size of the mouse and the position of the tumour. Despite the difficulties, the evaluation of the optical properties gave reasonable results.

There are many possible improvements in order to more accurately measure the optical properties. The most important is to have a realistic geometry coupled to a forward model based on a FEM or a Monte Carlo calculation. The geometry should include the geometry of the leg with the tumour, and the fibre positions.

The question that must be asked is if it is reasonable to develop and perform advanced measurements and evaluations for the mouse study. How accurate can the optical properties be estimated, will the result be better than if the optical properties from the literature is used?

Even if I am not sure that the development of a more advanced dosimetry would be of value for the mouse study, such a development can be an opportunity to gain experience that will be useful when proceeding to trials on humans. In PDT, the development of an individualized dosimetry is often mentioned as a necessity for the impact of the technique. I think that sooner or later, the PCI technique will be developed to a point where advanced dosimetry is necessary to proceed further.

8.1 Eurostars project

In the Eurostars project, WP3 is still going on. The current main goal is to understand which light doses that lead to PCI and PDT effect, respectively. For PCI, the highest dose not giving a PDT effect is sought. The group in Norway is performing the preclinical trials and Spectra Cure is helping with the evaluation of the light doses actually given. When the mechanism is better understood and the dose window is known, the PCI-technique will be tested with siRNA.

PCI Biotech is, outside the scope of the Eurostars project, currently performing a phase one clinical trial on superficial tumours in humans. In the last part of the Eurostars project, the goal is to test the PCI-technique on tumours inside the body. It is not yet decided whether to treat pancreas cancer or cancer in the ENT-region (ear, nose, throat). Interstitial fibres must be used and a method to insert the fibres is to be developed by Spectra Cure.

In an ongoing study on treating pancreas cancer with PDT CT is used. The insertion process is interrupted several times, and a CT scan is performed to check where the fibres are. Performing repetitive CT results in high radiation doses and an alternative method combines CT with ultrasound to minimize the radiation dose although the contrast remains high.

Acknoledgements

I have appreciated to work with this master thesis and to get an insight in Spectra Cure as a company and into the research field of PDT and PCI. I would like to thank the people at SpectraCure and at the atomic division who made it possible, especially I would like to thank my supervisors, Johannes Swartling and Stefan Andersson-Engels. I would also like to thank my colleagues in the same office, Joan Sandberg and Christofer Hellberg, for the company, bad jokes and the nice coffee breaks. At the atomic physics, I appreciated the help in the lab from Dmitry Khoptyar and Erik Alerstam.

Many thanks to Johan Ylikiiskil who has been a patient listener through both challenges and progress, and of course many thanks to my friends and family!

Bibliography

[1] J. Mobley and T. Vo-Dinh., *Biomedical Photonics Handbook.* CRC Press Boca Radon, USA, 2005. 6

[2] J. Axelsson, *Model-based Approaches to Diffuse Optical Imaging and Dosimetry.* PhD thesis, Lund institute of technology, 2009. 6, 13, 14, 15, 21

[3] A. Johansson, *Spectroscopic Thechniques for Photodynamic Therapy Dosimetry.* PhD thesis, Lund University, 2007. 6

[4] R. Haskell, L. Svaasand, T.-T. Tsay, T.-C. Feng, M. McAdams, and B. Tromberg, "Boundary conditions for the diffusion equation in radiative transfer," *Journal of the Optical Society of America A*, vol. 11, no. 10, pp. 2727 2741, 1994. 8, 23, 28

[5] A. Hielscher, S. Jacques, L. Wang, and F. Tittel, "The influence of boundary-conditions on the accuracy of diffusion-theory in time-resolved reflectance spectroscopy of biological tissues.," *Physics in medicine and biology*, vol. 40, pp. 1957 1975, 1995. 8

[6] A. Kienle and M. Patterson, "Improved solutions of the steady-state and the time-resolved diffusion equations for reflectance from a semi-infinite turbid medium.," *JOSA A*, vol. 14, pp. 246 254, 1997. 8

[7] S. A. Prahl, M. Keijzer, S. L. Jacques, and A. J. Welch, "A monte carlo model of light propagation in tissue," 2009. 9

[8] E. Alerstam, T. Svensson, and S. Andersson-Engels, "Parallel computing with graphics processing units for high-speed monte carlo simulation of photon migration.," *Journal of Biomedical Optics*, vol. 13, no. 6, pp. 60504 60505, 2008. 9

[9] E. Alerstam, S. Andersson-Engels, and T. Svensson, "Improved accuracy in time-resolved diffuse reflectance spectroscopy," *Opt Express*, vol. 16, pp. 10440 10454, 2008. 11

[10] I. Wang, *Photodynamic therapy and laser-based diagnostic studies of malignant tumours.* PhD thesis, 1999. 13

[11] A. Johansson, J. Axelsson, and S. Andersson-Engels, "Realtime light dosimetry software tools for interstitial photodynamic therapy of the human prostate.," *Medical Physics*, vol. 34, no. 11, pp. 4309 4322, 2007. 13

[12] I. Mellman, "Endocytosis and molecular sorting.," *Annual Review of Cell & Developmental Biology*, vol. 12, no. 1, pp. 575 626, 1996. 14

[13] O. Norum, P. Selbo, A. Weyergang, K. Giercksky, and K. Berg, "Photochemical internalization (pci) in cancer therapy: From bench towards bedside medicine," *Journal of Photochemistry and Photobiology B: Biology*, vol. 96, no. 2, pp. 83 92, 2009. 14, 15

[14] J. Moan and K. Berg, "The photodegradation of porphyrins in cells can be used to estimate the lifetime of singlet oxygen," *Photochem. Photobiol.*, vol. 53, pp. 549 553, 1991. 14

[15] A. Hogset, L. Prasmickaite, P. Selbo, M. Hellum, B. Engesaeter, A. Bonsted, and K. Berg, "Photochemical internalisation in drug and gene delivery," *Advanced Drug Delivery Reviews*, vol. 56, no. 1, pp. 95 115, 2004. 16

[16] Y. Censor, M. D. Altschuler, and W. D. Powlis, "On the use of cimmino's simultaneous projections method for computing a solution of the inverse problem in radiation therapy treatment planning," *Inverse problems : an international journal of inverse problems, inverse methods and computerised inversion of data*, vol. 4, no. 3, pp. 607 623, 1988. 20

[17] H. Dehghani, M. E. Eames, P. K. Yalavarthy, S. C. Davis, S. Srinivasan, C. M. Carpenter, B. W. Pogue, and K. D. Paulsen, "Near infrared optical tomography using nirfast: Algorithm for numerical model and image reconstruction," *Communications in numerical methods in engineering.*, vol. 25, no. 6, pp. 711 732, 2009. 26

[18] G. Alexandrakis, R. Rannou Fernando, and F. Chatziioannou Arion, "Tomographic bioluminescence imaging by use of a combined optical-pet (opet) system: a computer simulation feasibility study," *Physics in medicine and biology*, vol. 50, no. 17, pp. 4225 4241, 2005. 28, 37, 39, 40, 41

[19] J. Swartling, *Biomedical and atmospheric applications of optical spectroscopy in scattering media.* PhD thesis, Lund Institute of Technology, 2002. 32, 33